American Mineralogist, Volume 71, pages 1527–1541, 1986

Measurement of water in rhyolitic glasses: Calibration of an infrared spectroscopic technique

Sally Newman, Edward M. Stolper, Samuel Epstein
Division of Geological and Planetary Sciences, California Institute of Technology, Pasadena, California 91125, U.S.A.

Abstract

A series of natural rhyolitic obsidians were analyzed for their total water contents by a vacuum extraction technique. The grain size of the crushed samples can significantly affect these analyses. Coarse powders must be used in order to avoid surface-correlated water. These analyses were used to calibrate infrared spectroscopic measurements of water in glass using several infrared and near-infrared absorption bands. We demonstrate that infrared spectroscopy can yield precise determinations of not only total dissolved water contents, but also the concentrations of individual H-bearing species in natural and synthetic rhyolitic glasses on spots as small as a few tens of micrometers in diameter.

Introduction

The importance of volatiles (e.g., water, carbon dioxide) in igneous processes is considered by most geologists to be beyond serious question. One direct approach to evaluating the roles and behaviors of volatiles is through the determination of their concentrations in young volcanic glasses (e.g., Friedman and Smith, 1958; Craig and Lupton, 1976; Delaney et al., 1978; Killingley and Meunow, 1975; Pineau and Javoy, 1983; Taylor et al., 1983) and in glasses trapped as inclusions in phenocrysts (Harris, 1981; Harris and Anderson, 1983, 1984).

Although widely used by glass scientists for the measurement of "water" dissolved in silicate glasses, infrared (IR) spectroscopy has not been extensively used for this purpose by geologists. As usually practiced, this technique consists of measuring the intensity of IR radiation absorbed by a plate of glass of known thickness at an energy corresponding to a vibration of an H-bearing species. By Beer's law, the intensity of the absorption is proportional to the number of absorbers per unit area in the light path. Provided that the constant of proportionality (the extinction coefficient or molar absorptivity) between the number of absorbers per unit area and the intensity of absorption for the absorption band is known, the concentration of the absorbing species in the glass can be readily determined.

The IR technique has several features that are desirable from the point of view of the geologist interested in natural or synthetic hydrous glasses: (1) it is nondestructive; (2) the IR beam can be aimed at spots as small as a few tens of micrometers in diameter, thereby avoiding crystals, vesicles, or alteration; (3) the concentrations of individual species can be measured in addition to the total dissolved water content; and (4) it has a large range (from a few parts per million to tens of weight percent). Its principal disadvantages are that it requires preparation of polished samples of uniform thickness, and it must be calibrated relative to some absolute method. The IR technique must be calibrated for each composition of interest, and its sensitivity to minor variations in glass chemistry, water content, and thermal history is not well known.

In this study, we have evaluated the IR technique as applied to the determination of the water contents of rhyolitic glasses. We first determined the total water contents of a series of natural rhyolitic obsidians using the standard method whereby volatiles are extracted from the glass at high temperature under vacuum and all of the evolved water is converted into H_2, the volume of which is measured manometrically. This technique is widely used in laboratories that study D/H ratios of geologic materials (e.g., Friedman and Smith, 1958; Epstein and Taylor, 1970; Craig and Lupton, 1976; Knauth and Epstein, 1982; Taylor et al., 1983; Yang and Epstein, 1983). Using samples whose water contents had been determined in this way as standards, extinction coefficients for several IR absorption bands were then determined. By comparing the IR measurements with the manometric measurements, we have been able to evaluate the strengths and limitations of both techniques for measuring the water contents of glasses.

Sample description

The samples used in this study were rhyolitic obsidians from a variety of locations (Table 1). Some were from tephra deposits, and others were from domes and flows. Most were not clear glasses, but contained microvesicles and microphenocrysts. A few were banded with layers of clear and cloudy glass, the latter probably the result of high concentrations of microvesicles.

Methods

Manometry and D-H mass spectrometry

Sample preparation. Each glass was coarsely crushed to millimeter-sized fragments with a stainless-steel mortar and pestle and rinsed with acetone to remove dust from the surfaces. The crushed sample was examined under a binocular stereoscope;

0003–004X/86/1112–1527$02.00

Table 1. Sample locations, sources, and manometrically determined total water concentrations

Sample*	Location**	Source†	Total H_2O concentration‡ (wt%)	Sample size (g)	Total H_2O extracted (μmol)
BGM8-II-3 (1a and 2a)	1	1	0.367 ± 0.020§		
CIT-1 (1e)††	2	2	0.138 ± 0.003	2.1202	164.60
CIT-1 (2f)	2	2	0.164 ± 0.001	1.0404	95.15
DC-1 (1c)	3	3	0.275 ± 0.005	0.2702	43.05
DC-2 (1c)	3	3	0.121 ± 0.003	0.4174	29.93
GM3A2-0 (1a)	1	1	0.439 ± 0.006	0.2342	58.91
GM83-13 (1a)	1	4	1.03 ± 0.03	0.0248	16.01
KS (1b)	4	5	0.78 ± 0.01	0.1527	67.81
LGM-1a (1a)	5	1	0.68 ± 0.04	0.0191	9.06
MC84-bb-3a (1a)	4	6	(2.60 ± 0.03)	0.1549	225.42
MC84-bb-3b (LT)	4	6	1.77 ± 0.03	0.0472	48.34
MC84-bb-3b (1a)	4	6	1.32 ± 0.03	0.0475	36.72
MC84-bb-3c (1a)	4	6	1.59 ± 0.05	0.0153	15.34
MC84-bb-3d (1a)	4	6	(1.51 ± 0.01)	0.1160	99.31
MC84-bb-3e (1a)	4	6	(1.262 ± 0.009)	0.1489	106.14
MC84-bb-4b-b (1a)	4	6	(2.64 ± 0.02)	0.0551	82.61
MC84-bb-4b-r (1a)	4	6	(0.921 ± 0.007)	0.2096	109.00
MC84-bb-4g (1a)	4	6	(0.943 ± 0.005)	0.2948	156.23
MC84-bb-5j (1a)	4	6	(0.664 ± 0.010)	0.0753	29.58
MC84-bb-5m (1a)	4	6	(0.570 ± 0.007)	0.1981	64.56
MC84-df (1a–1f)	4	6	0.696 ± 0.004§§		
MC84-t (1a and 1b)	4	6	0.779 ± 0.005§		
N. Coulee (1a)	4	6	0.271 ± 0.002	0.7087	108.27
Upper dome, NW Coulee (1a)	4	6	0.294 ± 0.003	0.4761	79.44
NC5-V (1a)	6	1	(0.712 ± 0.009)	0.1461	59.59
NRO (1a)	6	8	0.076 ± 0.002	0.6461	29.10
PAN-82-bt (1a)	4	5	0.817 ± 0.014	0.1133	53.21
PAN-82-bv (1a)	4	5	0.224 ± 0.004	0.4445	57.16
Panum dome (1a)	4	6	0.119 ± 0.002	0.6005	41.49
POB-82-2 (AF)	4	5	1.84 ± 0.02	0.0744	77.79
POB-82-2 (D2, 3)	4	5	1.70 ± 0.03	0.0518	50.83
POB-82-45 (1a)	4	5	(0.983 ± 0.013)	0.3685	203.55

* Notations in parentheses identify fragments or aliquots used for particular analyses.

** Locations of samples: 1—Glass Mountain, Medicine Lake Highlands, California. 2—Coso Range, California. 3—Valles Caldera, New Mexico. 4—Mono Craters, California. 5—Little Glass Mountain, Medicine Lake Highlands, California. 6—Newberry crater, Oregon.

† Sources of samples: 1—H Westrich, Sandia Laboratories. 2—S. Epstein, California Institute of Technology. 3—I.S.E. Carmichael, University of California, Berkeley. 4—T. Grove, Massachusetts Institute of Technology. 5—K. Sieh, California Institute of Technology. 6—S. Newman, E. Stolper, S. Epstein, California Institute of Technology. 7—M. Bursik, California Institute of Technology. 8—A. T. Anderson, Jr., University of Chicago.

‡ Manometric determinations: Values in parentheses indicate that the chip used for manometry was *not* the same one or from the same fragment as that used for IR spectroscopy. Unless noted otherwise, all samples were crushed to 150–500 μm and run in batch mode.

†† Chips run stepwise.

§ Average of 2 runs.

§§ Average of 6 runs.

and fragments were hand-picked, avoiding any visible alteration (e.g., surface hydration), vesicles, and phenocrysts when possible. Finally, the picked glass was crushed further and sieved to various size fractions. Samples used for calibration of the IR technique were limited to the 150–500-μm size fraction or were run as >1-mm chips.

Extraction of water. The water was extracted by heating the sample in a covered Pt crucible with an induction furnace in a vacuum line similar to that described by Epstein and Taylor (1970). The extraction technique included preheating the Pt crucible in vacuum prior to loading the sample in order to remove any water in the crucible. This preheating by induction also eliminates water from the inside of the enclosing Pyrex chamber as it is heated by radiation from the glowing Pt. Temperatures greater than the maximum extraction temperature were reached during preheating. The sample and the sealed degassed chamber containing the Pt crucible were placed in an N_2 atmosphere in a P_2O_5 dry-box where the glass sample was loaded into the crucible and the chamber resealed. It was then removed from the dry-box and connected to the extraction line. After evacuation of the dry air, the induction furnace was turned on and the sample heated to the required temperatures. Samples run for total water concentration were heated slowly, over a period of 30–120 min, to ~1200°C. This maximum temperature was maintained for at least 15 min, or until no more evolving gas could be detected by the vacuum gauge. The temperature achieved in the sample chamber was calibrated at the high end (850–1000°C) using the temperature dependence of the vapor pressure of CuO (Dushman, 1949) and extended up to 1300°C using an optical pyrometer. At low temperatures, calibrations were done with a mercury thermometer (50–160°C) and by monitoring the melting point of metallic lead (327.5°C). The water emitted passed through a quartz

tube containing CuO kept at 500°C to oxidize any H_2 gas that may have been released from the sample. The total water was trapped in a liquid-N_2-cooled U-tube, and traces of noncondensables were pumped away. After the water was collected, the U-tube was warmed to dry-ice temperature and any released CO_2 was pumped away or collected for analysis. The water was then vaporized by warming the trap to room temperature followed by some gentle torching of the U-tube with a heat gun to insure the complete release of the water. The water was then passed over hot U metal for conversion to H_2. The gas was collected into a Toepler pump, where the amount was measured manometrically.

The precision of our measurements depends almost entirely on the amount of H_2 that is available for analysis, because it is determined by the precision of the manometric measurements and the precautions that are taken to eliminate background waters. In our laboratory we sometimes reduce our background to a fraction of a micromole and get high precisions by using special extraction lines (Yang and Epstein, 1983); this was not deemed necessary for this study, and the blank for the samples reported on here is approximately two micromoles. For routine measurements with the extraction procedure used here, a 20 micromole sample could be measured to ±2%, because the blank is reproducible to ±10%. Most of our samples were larger (Table 1) and the error was smaller.

D/H isotopic ratios. In some cases it was necessary to determine the hydrogen isotopic ratios of water released at different temperatures. This was done by stepwise heating of the samples, collecting the water released at various temperatures. In this way it was possible to monitor water adsorbed on surfaces (e.g., Epstein and Taylor, 1970). The δD values are measured mass spectrometrically using H_2 as the sample gas. The purity of the H_2 was routinely confirmed in the mass spectrometer.

The isotopic composition is expressed using the usual δ notation:

$$\delta D_{SMOW} = \left(\frac{(D/H)_s}{(D/H)_0} - 1 \right) \times 1000,$$

where the subscript s represents the sample and subscript 0 represents the reference standard, Standard Mean Ocean Water. The error of routine δD measurements is ±1‰.

Infrared spectroscopy

The experimental procedures followed were basically similar to those used by Stolper (1982). Since that time, some modifications of the techniques have been made.

Sample preparation. Obsidian fragments were mounted in orthodontic resin (L. D. Caulk Co.) and attached to microscope slides with acetone-soluble adhesive (Crystalbond 509, Aremco Products, Inc.) for grinding and polishing. Doubly polished plates of glass were prepared by grinding and then polishing with alumina abrasive using water as a lubricant or with diamond paste (Metadi compounds, Buehler Ltd.) using cutting fluid (Isocut, Buehler Ltd.) as a lubricant. Final polishing was done with 0.3–1.0-μm abrasive. Polished samples were cleaned in acetone or toluene. Most samples were stored in air. In some cases, the polished glass fragments analyzed by IR spectroscopy were also analyzed for total dissolved hydrogen by manometry as described above.

For most samples, spectra were obtained both in the IR and in the near-infrared (NIR) regions of the spectrum. Because of the greatly different intensities of absorptions in these regions, samples should ideally be 10–20 times thicker for NIR measurements than for IR measurements. Whenever possible, a thick specimen was first prepared and its NIR spectrum taken; this same fragment or a portion of it was then ground to a much smaller thickness and the IR spectrum was taken on this thinner fragment. In this way, intensities of absorption bands in the two regions of the spectrum could be directly compared, and possible problems with sample heterogeneity were minimized. In some cases, the IR and NIR fragments were prepared from different fragments of the same chunk of obsidian.

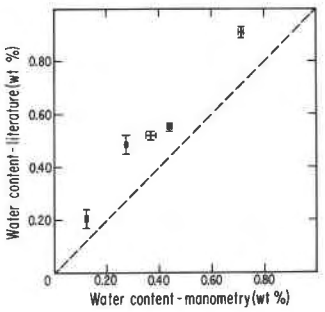

Fig. 1. The relationship between the water content reported in the literature and the values obtained by manometry for the same samples. The dotted line is the one-to-one relationship. Samples are NC5-V (P_2O_5 cell; Taylor et al., 1983), GM3A2-0 and BGM8-II3 (P_2O_5 cell; Westrich, pers. comm. in Stolper, 1982) and DC-1 and DC-2 (loss on ignition; Shaw, 1974). This figure shows the inconsistencies between the literature values and our data.

Infrared spectroscopy. Transmission spectra of the rhyolitic glasses were obtained between wavelengths of 1.3 and 8.0 μm. For each spectrum, the IR beam was "aimed" at a specific region of the glass plate by placing an aperture in a piece of brass or steel over the sample. For the spectra produced in this study, aperture sizes ranged from 200 to several thousand micrometers. Visible bubbles, crystals, and inclusions were avoided when possible by appropriate choice and placement of apertures.

A Cary 17 spectrophotometer was used to obtain spectra in the 1.3–2.7-μm region. The spectrometer and sample chamber were continuously purged with dried air. Spectra were recorded in a linear absorbance (base ten logarithm) mode versus wavelength on chart paper. These recordings are the basis of our quantitative measurements of absorbance.

A Perkin-Elmer model 180 spectrophotometer was used to obtain spectra in the 2.5–8.0-μm wavelength region. As for the NIR determinations, the spectrometer and sample chamber were continuously purged with dried air, and spectra were recorded in a linear absorbance (base ten logarithm) mode versus wavenumber on chart paper. For most samples, spectra were simultaneously collected with a Digital Equipment Corporation MINC-11 computer interfaced to the spectrophotometer. Quantitative absorbance measurements were nearly all based on the computer-collected data; in a few cases, quantitative measurements were based on hand-digitized versions of the chart recordings. A screen with known absorbance was used to verify the calibration of the spectrophotometer after every spectrum.

Results and discussion

Comparison of total water concentrations determined in this study with those determined by other techniques

Several of the rhyolitic obsidians that we have analyzed have also been analyzed for water by other investigators.

Table 2. Comparison of stoichiometric and measured water concentrations in hydrous minerals

Mineral	Chemical formula	Wt% H_2O stoichiometry	Wt% H_2O measured	CIT museum number and location
Diaspore	α-AlO(OH)	15.02	14.50 ± 0.16	1567; Chester, Massachusetts
Pyrophyllite	$Al_4[Si_8O_{20}](OH)_4$	5.00	4.98 ± 0.06	Mariposa County, California
Lawsonite	$CaAl_2(OH)_2[Si_2O_7]H_2O$	11.46	11.52 ± 0.13	2243; Tiburon Peninsula, California

Figure 1 shows that there are major differences between our manometric determinations and the water concentrations reported by other laboratories. In all cases the literature values are higher than the values determined in this study.

As shown in Table 2, in which we report water analyses for three minerals containing stoichiometric water (diaspore, pyrophyllite, and lawsonite), our technique does not systematically underestimate water contents. We have also been able to demonstrate, by obtaining IR spectra of glasses that have been melted during our extraction procedure, that essentially all of the dissolved water was extracted from the samples by this procedure. These results confirm that our extraction procedure and manometric measurements can provide accurate determinations of total water concentrations.

The success of our calibration of the IR technique is dependent on the accuracy of the manometric determinations of the total water contents of the standards. Given the discrepancies between our measurements and those from the literature (Fig. 1), we have tried to identify possible pitfalls in these sorts of analyses in order to design a recipe for reliable, routine water analysis that safely avoids them. Our conclusion is that surface-correlated water on crushed samples reported on in the literature is the likely cause of the discrepancies shown in Figure 1.

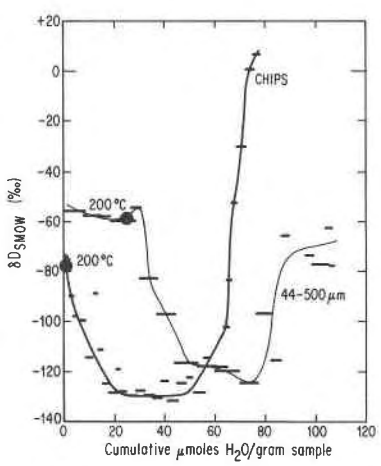

Fig. 2. A plot of the δD against the cumulative micromoles of H_2O extracted from 1 g of chips and 1 g of powdered (44–500 μm) CIT-1(1) samples by stepwise pyrolysis. The horizontal bars represent the individual extractions; the solid curves represent the smoothed spectra. The initial 30 μmol of water extracted from the 44–500-μm powders represents the surface-correlated water released at $\leq$200°C. The large dot on each curve represents the 200°C pyrolysis. The 44–500-μm fraction was held at $\leq$200°C for 167 min; the chips were held at $\leq$200°C for 450 min.

Investigation of surface-correlated water

The potential for absorption of water on the surfaces of crushed glass is well known. After all, hydration of obsidian surfaces occurs at relatively rapid rates (e.g., Friedman and Long, 1976; Michels et al., 1983). Knowledge of this led Friedman and Smith (1958) to study only coarse chips in their analyses of obsidians. Bryan and Moore (1977) quantified this effect for basaltic glasses by comparing water contents of coarsely and finely crushed MORB samples. Unfortunately, some recent workers have obtained water and D/H analyses on finely ground material (e.g., Eichelberger and Westrich, 1981; Taylor et al., 1983). Although this may offer some advantages, since it is more difficult and time-consuming to insure full extraction of water from coarser fragments, it probably results in inaccurate analyses. In this section, we try to establish the finest grain size that can be safely used without significant contribution from surface-correlated water and the necessary procedures for removing surface-correlated water.

We identified the presence of surface-correlated water by analyzing the water contents of two aliquots of sample CIT-1(1) with different grain sizes. One aliquot included particles 44–500 μm in size and the other consisted of 1–3-mm chips. The finer fraction sat exposed to laboratory air for ten days between crushing and analysis, whereas the chips sat for less than a day. The water in each aliquot was extracted stepwise as the temperature was increased in order to determine the isotopic compositions of successive fractions as they were extracted. The samples were held at each temperature until little additional gas was

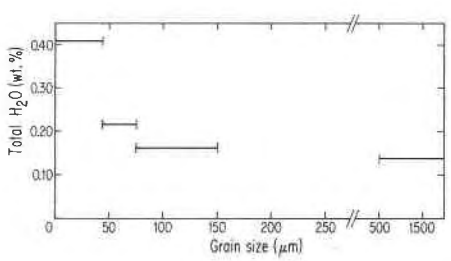

Fig. 3. Total water extracted from different grain-size fractions of sample CIT-1(1). The horizontal bars represent the size ranges of the grains in each sample.

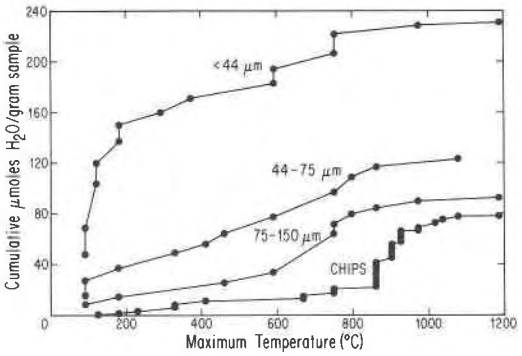

Fig. 4. Micromoles of H_2O extracted at different temperatures per gram of powder of different grain-size fractions of CIT-1(1) during stepwise pyrolysis. For extraction temperatures above ~200°C, all of the curves are approximately parallel, suggesting that surface-correlated water is almost completely removed below 200°C. The variations of the rates of H_2O extraction for the different powders reflect the surface-to-mass ratio of the grains.

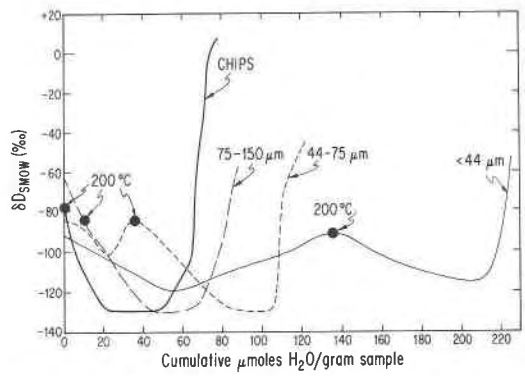

Fig. 5. A plot of the δD values against the cumulative micromoles of water extracted from four different samples. These samples are powders of <44, 44–75, and 75–150 μm, and chips all from sample CIT-1(1). This figure is similar to Figure 2. We do not show bars for the individual extractions, to prevent confusion. The large dot on each curve represents the 200°C pyrolysis. The length of time each sample was held at ≤200°C was 138 min for the <44-μm fraction, 137 min for the 44–75-μm fraction, 132 min for the 75–150-μm fraction, and 450 min for the chips. Note the increase of the proportion of surface water as grain size decreases.

being evolved. The relationship between the δD and cumulative micromoles of water extracted is shown in Figure 2 and shows that the finer-grained fraction contained significantly more water than the chips, 0.191 versus 0.138 wt% water. The patterns observed for the two extractions are similar, provided the water given off at temperatures of 200°C and below in the finer-grained sample is ignored. Subtracting this low-temperature fraction, which has a distinctive isotopic pattern, from the total water results in a value of 0.143 wt% for the fine-grained aliquot. This value compares favorably with the value of 0.138 wt% for the water content of the coarser glass chips.

In order to exaggerate the effects of surface water, several size fractions of the CIT-1(1) glass (<44 μm, 44–75 μm, 75–150 μm) were soaked in isotopically light (δD = −400‰) water for two days after sitting exposed to laboratory air for 97 days. After they were removed from the light water, these samples were stored in air for 4 to 19 days. These samples exhibit a large increase in total water content with decreasing grain size (Fig. 3). The results of stepwise pyrolysis of these samples are shown in Figures 4 and 5. Figure 4 verifies that at temperatures below 200°C, significant water is released only from the finer fractions and that the amount increases with decreasing grain size. That the water released below 200°C is indeed extraneous is verified in Figure 5 by the isotope analyses of the different steps. Above 200°C, the variation in δD with amount of emitted water is similar in all cases, including the coarse chips. This fact indicates that this water is intrinsic to the glass. Below 200°C, the δD values of the released water are erratic; we suggest that this is water added during crushing, exposure to air, and the soaking procedure. Surprisingly, this water is not particularly light, although it is lighter than the equivalent low-temperature fraction in the unsoaked fine-grained aliquot (Fig. 2); this may reflect back reaction between surface-correlated water and the laboratory atmosphere after the soaking procedure was completed.

Confirmation that the water released at temperatures greater than 200°C is primarily the intrinsic water of the glass comes from the observations for the two largest size fractions. These samples have 0.136 wt% water if only the >200°C fraction is considered (Table 3). For the finer powders, the water content of the >200°C fraction is 0.143–0.154 wt%, suggesting that for very fine grained materials even 200°C may not be enough to remove all surface-correlated water. The most practical suggestion is to avoid analyses of fine powders.

The observed increase in total water content with decreasing grain size (Fig. 3) is easily rationalized in terms of hydration of the grain surfaces. Water concentrations in hydrated obsidian are as high as 7 wt% (Lee et al., 1974; Jezek and Noble, 1978). Assuming this concentration in the hydrated layer, a "diffusion coefficient" for hydration of 40 $\mu m^2/10^3$ yr has been calculated for the 44–75-μm powder, assuming spherical grains with a diameter of 60 μm. This compares reasonably well with values at 25°C of 2–30 $\mu m^2/10^3$ yr extrapolated from higher temperatures by Friedman and Long (1976) and Michels and coworkers

Table 3. Measured total water content vs. content calculated by subtracting water extracted at ≤200°C

Sample CIT-1(1e)	Total water content measured (wt%)	Water content at >200°C (wt%)
Chips	0.138 ± 0.003	0.136 ± 0.003
75–150 μm	0.161 ± 0.003	0.135 ± 0.002
44–75 μm	0.216 ± 0.002	0.154 ± 0.002
≤44 μm	0.408 ± 0.005	0.146 ± 0.003
44–500 μm	0.191 ± 0.003	0.143 ± 0.003

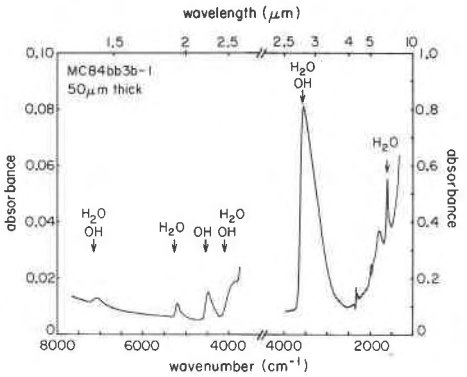

Fig. 6. Infrared spectrum of rhyolitic obsidian MC84bb-3b(1), scaled to a thickness of 50 μm. The absorbance scale on the left side of the figure refers to the low-wavelength portion of the spectrum; the absorbance scale on the right refers to the high-wavelength portion shown at the right. Absorption bands due to H-bearing species are indicated with arrows.

(1983). The agreement of these values suggests that the excess water in fine-grained powders results from actual diffusion of water into the glass and not just development of monolayers on the surfaces.

Our principal conclusion is basically common sense: avoid powdered materials if at all possible. If crushing is necessary, the time that elapses between crushing and analysis should be kept to a minimum. We emphasize that efforts to remove adsorbed water by heating at ~110°C are not likely to be entirely effective; indeed, we have shown that 200°C may not be sufficient for removal of extraneous water from fine-grained samples. The details of how surface-correlated water behaves are likely to be a function of glass chemistry, and our results may not apply to other systems. In particular, in water-rich systems in which the diffusivity of "water" is dramatically increased over water-poor obsidians, intrinsic water probably begins to be removed at temperatures near 100°C, in which case efforts to remove extraneous water would probably interfere with the analysis of the intrinsic water.

The procedure that we adopted for the glasses used for calibrating the infrared technique is as follows: Analyses were typically performed on 150–500-μm fragments stored in vacuum. This grain size was chosen as a compromise between the desire to minimize both the extraction times and the adsorbed water component. We examined the necessity for preheating at this grain size by comparing the δD values and bulk water concentrations of several samples that had not been preheated against those obtained on samples that had been preheated to 150°C for approximately 5.5 h. The 150°C heating had little effect on the δD values or water concentrations in samples with between 0.13 and 1.26 wt% water (Table 4), although the glass containing the most water (1.26 wt%) may have lost some water on preheating. This loss may have been intrinsic water since obsidian with this water content contains significant amounts of dissolved H_2O molecules which can be lost at much lower temperatures than OH groups. However, it is also possible that this loss was surface-correlated water. In any case, the loss is small, at most a few percent of the total water present. In addition, a 150–500-μm aliquot of the CIT-1(1) sample gave the same concentration of water after 150°C preheating as after the 200°C preheating for the large chips. The glasses analyzed for the IR calibration were 150–500-μm fragments stored in vacuum and were generally not preheated to remove adsorbed water, as a compromise between the avoidance of surface-correlated water and retaining all intrinsic water in the glasses.

Infrared spectra of hydrous rhyolitic glasses

Band assignments. Figure 6 shows a typical spectrum of a natural rhyolitic obsidian over the wavelength range that we have examined. Note the change of scale between the low- and high-wavenumber regions of the spectrum. This reflects the much greater intensities of the absorption bands at higher wavelengths in the IR relative to those at lower wavelengths in the NIR.

For the most part, the band assignments are straightforward (Stolper, 1982). The broad asymmetric band that peaks at ~3570 cm^{-1} is attributed to the fundamental OH-stretching vibration (Nakamoto, 1978). Its breadth and asymmetry, which are functions of the distribution of H-bond strengths within the glass, appear to be essentially identical in all of the rhyolitic glasses that we have studied, regardless of total water content. The band at ~7100 cm^{-1} is the first overtone of the OH-stretching vibration (e.g., Bartholomew et al., 1980); at the highest water contents, a shoulder appears at ~6800 cm^{-1}, perhaps related to clustered water molecules. The approximately symmetrical band at ~1630 cm^{-1} is due to the fundamental bending mode of water molecules (Nakamoto, 1978). The band at ~5200 cm^{-1} is produced by the combination stretching + bending mode of water molecules (Scholze, 1960; Bartholomew et al., 1980). The band at ~4500 cm^{-1} is assigned to combination modes

Table 4. Comparison of results of aliquots run with and without preheating

Sample	No preheating		After ~150°C preheating			After ~200° preheating for 2 h	
	H_2O (wt%)	δD_{SMOW} (‰)	H_2O (wt%)	δD_{SMOW} (‰)	Time (h)	H_2O (wt%)	δD_{SMOW} (‰)
CIT-1(1)	0.141 ± 0.002		0.138 ± 0.002			0.136 ± 0.001	
CIT-1(2)	0.167 ± 0.006	−121.1	0.164 ± 0.001	−122.3	5.6	0.170 ± 0.002	−121.6
MC84-df(1)	0.696 ± 0.004	−69.1	0.689 ± 0.003	−69.2	4.8	0.679 ± 0.008	−69.2
MC84-bb-3e(1)	1.262 ± 0.009	−62.3	1.242 ± 0.005	−64.8	5.5	not determined	

Note: Grain size = 150–500 μm.

of Si–OH and probably Al–OH groups (Scholze, 1966; Stolper, 1982). Other *X*–OH groups may also absorb in this wavenumber range. The only major band whose assignment is uncertain is at ~4000 cm^{-1}. It has been variously assigned to combination modes of strongly H-bonded silanol groups (Wu, 1980), to vibrations involving both water molecules and hydroxyl groups (Stolper, 1982), and to vibrations involving only dissolved water molecules (Acocella et al., 1984). A minor band at ~5600 cm^{-1} appears to be correlated with the intensity of the molecular water band at 5200 cm^{-1}. It may represent an additional combination mode for water molecules; liquid water has a similar band at ~5634 cm^{-1}.

Several other absorption bands are observed in rhyolitic obsidians over the wavelength range that we have studied. The bands at ~2000 cm^{-1} and 1800 cm^{-1} and the rising background to lower wavenumbers shown in Figure 6, plus a band at 1600 cm^{-1} (not discernable in Fig. 6) are attributed to vibrations of the aluminosilicate portions of the glass. That these bands are not related to H-bearing species in the glasses is confirmed by the fact that the bands shown by anhydrous glass prepared by vacuum fusion of natural obsidians are of the same intensities as those shown by natural obsidians whose dissolved water contents span the entire range that we have studied.

The noise at ~2350 cm^{-1} is due to incomplete purging of CO_2 from the spectrometer. When the spectrometer is carefully purged with dry N_2, the noise in this region is eliminated, and a very small band at ~2348 cm^{-1} remains in the water-rich natural glasses. This is probably due to dissolved molecules of CO_2. Based on the extinction coefficient given in Fine and Stolper (1985) for this band in sodium aluminosilicate glasses, the maximum concentration of molecular CO_2 in the glasses that we have studied is about 30 ppm by weight.

Absorbance and integrated absorbance measurements. Measurements of the intensities of absorption bands for the six bands for the glass samples studied by us are listed in Tables 5 and 6. We typically only determined the peak height (=absorbance) of a band, but for many samples the area of the band (=integrated absorbance) was also determined. Also given in these tables are the thicknesses and densities of the glasses. The precise locations of the peaks of some of the bands are also given in these tables.

For the bands in the IR (3570 cm^{-1} and 1630 cm^{-1}), all quantitative measurements are based on computer-collected data, smoothed using a procedure similar to that of Savitsky and Golay (1964). For the bands in the NIR (7100 cm^{-1}, 5200 cm^{-1}, 4500 cm^{-1}, 4000 cm^{-1}), most measurements are simple absorbance measurements and were taken directly from the chart recordings. Some measurements were based on digitized data as described in Stolper (1982).

One of the uncertainties in our absorbance measurements is in the background-subtraction procedure. For the fundamental OH-stretch band at 3570 cm^{-1}, the background is essentially flat, so a linear background tangent to the observed spectrum at about 3800 cm^{-1} and 2500 cm^{-1} was assumed.

For the band due to bending of H_2O molecules at 1630 cm^{-1}, the background is complicated because of the aluminosilicate bands in the vicinity, especially the one at 1600 cm^{-1}. For this band, the spectrum of a vacuum-melted sample of POB-82-45 was computer-subtracted from each spectrum, leaving an approximately flat background plus a band centered at 1630 cm^{-1}. The measurements of band intensity listed in Table 6 are based on such computer-subtracted spectra. This procedure is not without uncertainties, and slightly different band intensities are obtained if the background subtraction is based on other anhydrous glass spectra.

The background for the NIR bands has contributions from the high-energy tail of the fundamental OH band and from absorptions due to dissolved Fe (Stolper, 1982). In the case of digitized data, the background was modeled as described in Stolper (1982) and computer-subtracted from the data. However, this procedure is cumbersome, so we adopted the graphical procedure of simply drawing a linear or curved background that is tangent to the spectrum on either side of each band. A French curve was used in most cases. On the basis of repeated measurements of band intensities in this way by different people on the same samples over several years, we conclude that for all but the 4000-cm^{-1} band, negligible imprecision is contributed to our measurements by the subjective nature of background assignments for bands in the NIR. The 4000-cm^{-1} band sits on the tail of the fundamental OH-stretch band at 3570 cm^{-1} so its background is strongly sloped and curved, making precise measurement of its intensity difficult. We have therefore made little effort to study this band quantitatively beyond what was reported in Stolper (1982).

Precision of absorbance and integrated absorbance measurements. One of our major concerns has been the precision of our measurements of absorption-band intensities. We base our estimates of the precision of the measurements on the reproducibility of measurements on specific glass fragments made repeatedly over periods of up to several years. Polished glass fragments were stored in the laboratory in air between measurements. For most of these repeated measurements, the samples were replaced over the aperture for each measurement and the aperture size and placement were usually not identical for each spectrum. Thus, our estimates of precision may include uncertainties due to possible reaction of the samples with the atmosphere between analyses, to the effects of variable aperture size and placement, to possible sample heterogeneities, as well as to the precision of the spectrometer itself and our background-subtraction procedure.

We estimate that the typical uncertainty in our absorbance measurements for the fundamental OH-stretch band at ~3570 cm^{-1} is less than 0.02 absorbance units; i.e., better than 2% at an absorbance of 1 or 4% at an absorbance of 0.5. The reproducibility of our measurements is often much better than this; deviations of greater than 0.015 absorbance units between different measurements of the same sample are rare. Beer's law tests (i.e., measurements of absorption per unit thickness on fragments

Table 5. Data on IR bands

Sample	d (cm)*	Density** (g/L)	3570-cm⁻¹ band abs†	3570-cm⁻¹ band int-abs†† (cm⁻¹)	3570-cm⁻¹ band Peak (cm⁻¹)	1630-cm⁻¹ band abs†	1630-cm⁻¹ band int-abs†† (cm⁻¹)	1630-cm⁻¹ band Peak (cm⁻¹)
BGM8-III (3a)	0.0135	2380	0.63‡	289	3573	—‡‡	—‡‡	—‡‡
CIT-1 (1a)	0.0270	2350	0.47	207	3574	n.d.	n.d.	n.d.
CIT-1 (1c)	0.0120	2350	0.20	n.d.	n.d.	n.d.	n.d.	n.d.
CIT-1 (1d)	0.0130	2350	0.22	n.d.	n.d.	n.d.	n.d.	n.d.
CIT-1 (2g)	0.0180	2360	0.34	152	3573	n.d.	n.d.	n.d.
DC-1 (1a)	0.0149	2350	0.59‡	267	3579	n.d.	n.d.	n.d.
DC-2 (1a)	0.0211	2360	0.36‡	158	3578	—‡‡	—‡‡	—‡‡
GM83-13 (1b)	0.0068	2360	0.82	373	3569	0.15	7.7	1634
KS (1a1)	0.0072	2330	0.67	300	3562	0.12	5.4	1632
KS (1a2)	0.0074	2330	0.66	298	3572	0.11	5.0	1632
LGM-1a (2a)	0.0066	2360	0.65‡	302	3559	0.08	3.8	1629
MC-84-bb-3a (2a)	0.00285	2280	0.74	326	3580	0.27	12.9	1631
MC-84-bb-3b (LT)	0.0050	2310	0.91	403	3579	0.27	12.9	1631
MC-84-bb-3b (1a)	0.0058	2300	0.84	370	3577	0.19	8.8	1632
MC-84-bb-3c (1a)	0.0062	2310	1.05	465	3570	0.27	12.2	1632
MC-84-bb-3d (2a)	0.0063	2320	0.97	429	3578	0.25	12.3	1632
MC-84-bb-3e (2a)	0.0068	2320	0.98	422	3569	0.21	9.0	1632
MC-84-bb-4b-b (2a)	0.0042	2280§	1.07	469	3564	0.41	19.8	1630
MC-84-bb-4b-r (2a)	0.0111	2340	1.05	458	3578	0.17	8.0	1634
MC-84-bb-4g (2a)	0.0111	2340	1.08	471	3580	0.15	7.3	1632
MC-84-bb-5j (2a)	0.0155	2310	1.04	458	3583	0.06	2.7	1639
MC-84-bb-5m (2a)	0.0104	2330§	0.90	401	3566	0.10	5.0	1633
MC-84-df (1a)	0.0109	2350	0.77	348	3570	0.08	4.2	1633
MC-84-t (1a)	0.0112	2330	0.95	420	3569	0.17	8.1	1633
N. Coulee (1b)	0.0169	2340	0.52	231	3575	0.04	3.3	1639
N. W. Coulee (1b)	0.0183	2340	0.62	268	3575	0.07	6.0	1641
NC5-V (3a)	0.0081	2380	0.67‡	304	3566	0.07	3.1	1632
NRO (1b)	0.0150	2380	0.16	68	3565	—‡‡	—‡‡	—‡‡
OBS-E (1a)	0.0040	2340§§	0.77‡	353	3575	0.22	9.7	1636
OBS-G (1a)	0.0042	2340§§	0.97‡	443	3573	0.32	15.9	1629
OBS-I (1a)	0.0015	2330§§	0.53‡	233	3584	n.d.	n.d.	n.d.
PAN-82-bb-3c (2a)	0.0042	2310	0.84	381	3582	0.27	13.0	1631
PAN-82-bt (1b)	0.0083	2340	0.78	340	3582	0.15	7.0	1632
PAN-82-bv (1b)	0.0291	2330	0.92	392	3570	n.d.	n.d.	n.d.
Panum Dome (1b)	0.0178	2350	0.27	120	3581	n.d.	n.d.	n.d.
POB-82-2 (B)	0.0056	2330	1.01	459	3575	0.29	14.4	1632

Note: n.d. = not determined.

* Thicknesses (*d*) of the polished glass plates were measured mostly with a digital dial indicator (543 Series Digimatic Indicator, Mitutoyo Mfg. Co., Ltd.) with a resolution of 1 μm. Based on repeated measurements of samples over several years, a precision of 1 μm in these measurements is estimated. We have no test of the accuracy of these measurements, but the manufacturer's specifications are ±2 μm, and our comparisons with measurements made with micrometers tend to support this. Some measurements are based on Stolper (1982) and were made with a micrometer. The real uncertainty in thickness measurements comes from the lack of parallelism of the two polished surfaces of the glass plates. Although not usually a major problem, since thickness was usually measured on the same spot at which the infrared beam was aimed, we estimate that errors as large as 3 μm may be more realistic than the 1-μm precision of the measuring device.

** Sample densities are required to convert the IR measurements into concentratons in weight percent. For nearly all samples, densities were measured using a Berman balance with toluene as the reference liquid. On the basis of repeated measurements of the density of a quartz grain with approximately the same mass as the glass fragments on which we measured density, a precision at the 1 sigma level of 0.15% is estimated. Actual glass densities are not known this well owing to the presence of bubbles, crystals, and inclusions in the natural glasses. We estimate an error of approximately 1% in our glass-density measurements.

† Absorbance; error: 0.01.

†† Integrated absorbance; error: 5%.

‡ Value differs from Stolper (1982). Based on digitized chart recording.

‡‡ Below detection limit.

§ Assumed.

§§ Calculated (Stolper, 1982).

of the same glass polished to different thicknesses) confirm that our absorption-coefficient measurements have uncertainties of less than a few percent (see Fig. 7) for this band. Integrated absorbance measurements appear to have similar levels of uncertainty.

A similar uncertainty of about 0.01 absorbance units is estimated for the H_2O-bending mode at ~1630 cm^{-1}. This corresponds to a larger relative error than for the stretching band at 3570 cm^{-1} because intensities are usually lower for the bending mode. Reproducibility for integrated absorbance measurements for this band appears to be worse by a factor of 2–3 than the absorbance measurements. We emphasize that offsets in the intensity of this band at least as large as those that we have observed between repeated spectra of a sample can be produced by different choices of background spectra. Thus, only by careful consideration of background shapes can results that are accurate to better than several percent be expected for this band unless band intensities are much higher than those we have studied.

Table 6. Data on NIR bands

Sample	*d* (cm)*	Density** (g/L)	7100-cm^{-1} band			5200-cm^{-1} band			4500-cm^{-1} band			4000-cm^{-1} band		
			abs†	int-abs (cm^{-1})	Peak (cm^{-1})	abs†	int-abs (cm^{-1})	Peak (cm^{-1})	abs†	int-abs (cm^{-1})	Peak (cm^{-1})	abs†	int-abs (cm^{-1})	Peak (cm^{-1})
BGM8-II3 (1a)	0.2610	2380	0.0550(150)	14.2	7018	0.0200(20)	5.6	5200	0.2000(20)	37.8	4521	0.144(10)	37.5	3923
CIT-1 (1b)	0.1135	2350	0.0050(20)	n.d.	n.d.	0.0000(20)	n.d.	n.d.	0.0332(10)	n.d.	n.d.	n.d.	n.d.	n.d.
CIT-1 (2g)	0.3755	2360	n.d.	n.d.	n.d.	0.0000(20)	n.d.	n.d.	0.1370(50)	n.d.	n.d.	n.d.	n.d.	n.d.
DC-1 (1b)	0.2590	2350	0.0280(120)	8.6	7072	0.0110(20)	1.6	5203	0.1480(20)	28.5	4519	0.110(10)	28.4	3939
DC-2 (1b)	0.4170	2360	0.0280(120)	8.5	7018	0.0000(20)	0	n.d.	0.1160(20)	23.4	4498	0.076(10)	19.7	3915
GM83-13 (1a)	0.0477	2360	0.0160(20)	n.d.	n.d.	0.0285(20)	n.d.	n.d.	0.0745(20)	n.d.	n.d.	n.d.	n.d.	n.d.
KS (1a)	0.0288	2330	n.d.	n.d.	n.d.	0.0129(20)	n.d.	n.d.	0.0397(20)	n.d.	n.d.	n.d.	n.d.	n.d.
LGM-1a (1a)	0.1462	2360	0.0420(20)	12.1	7072	0.0530(20)	8.9	5222	0.1800(20)	32.4	4515	0.156(10)	40.0	3931
MC-84-bb-3a (2a)	0.1226	2280	0.1020(20)	n.d.	n.d.	0.3665(20)	n.d.	n.d.	0.3318(20)	n.d.	n.d.	n.d.	n.d.	n.d.
MC-84-bb-3b (LT)	0.1570	2310	0.0930(20)	n.d.	n.d.	0.2550(20)	n.d.	n.d.	0.3520(20)	n.d.	n.d.	n.d.	n.d.	n.d.
MC-84-bb-3b (1a)	0.1267	2300	0.0575(20)	n.d.	n.d.	0.1220(20)	n.d.	n.d.	0.2420(20)	n.d.	n.d.	n.d.	n.d.	n.d.
MC-84-bb-3c (1a)	0.1186	2310	0.0635(20)	n.d.	n.d.	0.1500(20)	n.d.	n.d.	0.2520(20)	n.d.	n.d.	n.d.	n.d.	n.d.
MC-84-bb-3d (2a)	0.0809	2320	0.0365(20)	n.d.	n.d.	0.0868(20)	n.d.	n.d.	0.1525(20)	n.d.	n.d.	n.d.	n.d.	n.d.
MC-84-bb-3e (2a)	0.0554	2320	0.0265(20)	n.d.	n.d.	0.0545(20)	n.d.	n.d.	0.1090(20)	n.d.	n.d.	n.d.	n.d.	n.d.
MC-84-bb-4b-b (2a)	0.0324	2280††	0.0325(20)	n.d.	n.d.	0.0935(20)	n.d.	n.d.	0.0823(20)	n.d.	n.d.	n.d.	n.d.	n.d.
MC-84-bb-4b-*r* (2a)	0.0832	2340	0.0255(20)	n.d.	n.d.	0.0370(30)	n.d.	n.d.	0.1070(40)	n.d.	n.d.	n.d.	n.d.	n.d.
MC-84-bb-4g (2a)	0.0965	2340	0.0285(20)	n.d.	n.d.	0.0393(20)	n.d.	n.d.	0.1410(20)	n.d.	n.d.	n.d.	n.d.	n.d.
MC-84-bb-5j (2a)	0.0834	2310	0.0173(20)	n.d.	n.d.	0.0120(20)	n.d.	n.d.	0.0863(20)	n.d.	n.d.	n.d.	n.d.	n.d.
MC-84-bb-5m (2a)	0.0260	2330††	0.0060(08)	n.d.	n.d.	0.0085(08)	n.d.	n.d.	0.0370(20)	n.d.	n.d.	n.d.	n.d.	n.d.
MC-84-df (LT)	0.1449	2340	0.0325(20)	n.d.	n.d.	0.0435(20)	n.d.	n.d.	0.1730(20)	n.d.	n.d.	n.d.	n.d.	n.d.
MC-84-df (1a)	0.1290	2350	0.0283(20)	n.d.	n.d.	0.0400(20)	n.d.	n.d.	0.1530(20)	n.d.	n.d.	n.d.	n.d.	n.d.
MC-84-t (1a)	0.0816	2330	0.0233(20)	n.d.	n.d.	0.0370(20)	n.d.	n.d.	0.1000(20)	n.d.	n.d.	n.d.	n.d.	n.d.
N. Coulee (1b)	0.1235	2340	0.0143(13)	n.d.	n.d.	0.0069(06)	n.d.	n.d.	0.0667(47)	n.d.	n.d.	n.d.	n.d.	n.d.
N.W. Coulee (1b)	0.1682	2340	n.d.	n.d.	n.d.	0.0122(16)	n.d.	n.d.	0.0965(10)	n.d.	n.d.	n.d.	n.d.	n.d.
N.W. Coulee (LT)	0.2222	2320	n.d.	n.d.	n.d.	0.0200(20)	n.d.	n.d.	01395(10)	n.d.	n.d.	n.d.	n.d.	n.d.
NC5-V (2a)	0.2055	2380	0.0490(20)	13.3	7057	0.0700(20)	11.4	5203	0.2530(20)	45.9	4517	0.203(10)	51.2	3934
NRO (1b)	0.3730	2380	n.d.	n.d.	n.d.	0.0000(20)	n.d.	n.d.	0.0660(16)	n.d.	n.d.	n.d.	n.d.	n.d.
OBS-E (1a)	0.0465	2340‡	0.0310(20)	11.4	7082	0.0730(20)	10.1	5238	0.1020(20)	21.2	4531	0.127(10)	39.1	3928
OBS-G (1a)	0.0342	2340‡	0.0250(20)	8.2	7067	0.0710(20)	10.1	5247	0.0850(20)	15.7	4525	0.110(10)	32.3	3915
OBS-I (1a)	0.0250	2330‡	0.0300(20)	11.1	7062	0.1160(20)	16.0	5244	0.0690(20)	15.6	4513	0.134(10)	40.9	3956
PAN-82-bb-3c (3a)	0.1410	2310	0.0950(20)	n.d.	n.d.	0.2760(20)	n.d.	n.d.	0.3300(20)	n.d.	n.d.	n.d.	n.d.	n.d.
PAN-82-bt (1b)	0.0286	2340	n.d.	n.d.	n.d.	0.0148(20)	n.d.	n.d.	0.0349(20)	n.d.	n.d.	n.d.	n.d.	n.d.
PAN-82-bv (1b)	0.0540	2330	n.d.	n.d.	n.d.	0.0000(20)	n.d.	n.d.	0.0250(20)	n.d.	n.d.	n.d.	n.d.	n.d.
Panum Dome (1b)	0.3610	2350	n.d.	n.d.	n.d.	0.0000(20)	n.d.	n.d.	0.0940(30)	n.d.	n.d.	n.d.	n.d.	n.d.
POB-82-2 (AF)	0.1122	2330	0.0690(20)	n.d.	n.d.	0.1940(20)	n.d.	n.d.	0.2540(20)	n.d.	n.d.	n.d.	n.d.	n.d.
POB-82-2 (B)	0.0554	2330	0.0310(20)	n.d.	n.d.	0.0860(20)	n.d.	n.d.	0.1240(20)	n.d.	n.d.	n.d.	n.d.	n.d.
POB-82-2 (C)	0.0558	2330	0.0320(20)	n.d.	n.d.	0.0890(20)	n.d.	n.d.	0.1220(20)	n.d.	n.d.	n.d.	n.d.	n.d.
POB-82-2 (A0-2)	0.0645	2330	0.0360(20)	n.d.	n.d.	0.1040(20)	n.d.	n.d.	0.1420(20)	n.d.	n.d.	n.d.	n.d.	n.d.
POB-82-2 (D2-3)	0.0565	2330	0.0313(20)	n.d.	n.d.	0.0910(20)	n.d.	n.d.	0.1180(20)	n.d.	n.d.	n.d.	n.d.	n.d.
POB-82-2 (F1-0)	0.0575	2330	0.0315(20)	n.d.	n.d.	0.0825(20)	n.d.	n.d.	0.1218(20)	n.d.	n.d.	n.d.	n.d.	n.d.
POB-82-2 (F2-0)	0.0581	2330	0.0330(20)	n.d.	n.d.	0.0935(20)	n.d.	n.d.	0.1303(20)	n.d.	n.d.	n.d.	n.d.	n.d.
POB-82-2 (F3-0)	0.0575	2330	0.0333(20)	n.d.	n.d.	0.0925(20)	n.d.	n.d.	0.1265(20)	n.d.	n.d.	n.d.	n.d.	n.d.
POB-82-45 (A2)	0.0930	2340	0.0290(20)	n.d.	n.d.	0.0525(20)	n.d.	n.d.	0.1380(20)	n.d.	n.d.	n.d.	n.d.	n.d.
POB-82-45 (AF)	0.0954	2340	0.0230(20)	n.d.	n.d.	0.0260(20)	n.d.	n.d.	0.1190(20)	n.d.	n.d.	n.d.	n.d.	n.d.

Note: n.d. = not determined.

* Thickness (*d*); error: 0.0003 cm. See Table 5 footnote concerning thickness measurements.

** Error: 1%. Values based on measurements with Berman balance, unless otherwise indicated. See Table 5 footnote concerning density measurements.

† Numbers in parentheses indicate assigned errors, in units of last significant digit.

†† Assumed.

‡ Calculated (Stolper, 1982).

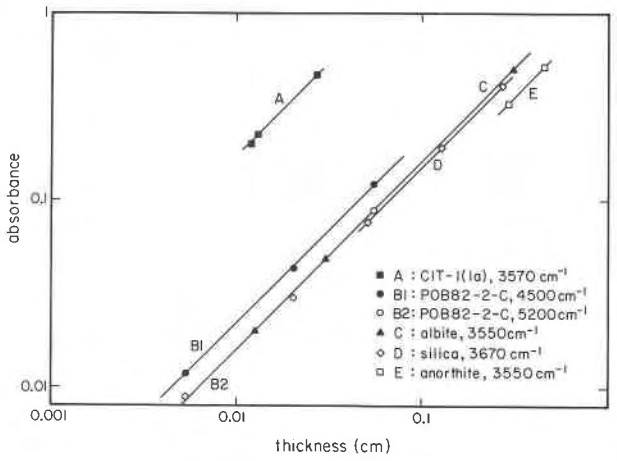

Fig. 7. Absorbance versus thickness for five silicate glasses. Each glass or absorption band falls on a 45° line, confirming Beer's law for these samples. Absorption-band locations are approximate.

Reproducibility in absorbance measurements in the NIR appears to be somewhat better in absolute terms than those in the IR, with differences between repeated measurements of band intensities seldom exceeding 0.003 absorbance units for the 7100-cm^{-1}, 5200-cm^{-1}, and 4500-cm^{-1} bands. In no case has a discrepancy as large as 0.01 absorbance units been observed. However, the relative errors in absorbance measurements are comparable to those of the 3570-cm^{-1} band because the band intensities tend to be smaller than those in the IR. For example, based on eight measurements of five different fragments of the MC84-df sample of different thicknesses, standard deviations of 3.6% for the 5200-cm^{-1} absorption coefficient and 1.1% for the 4500-cm^{-1} absorption coefficient were observed. Deviations of this sort between repeated measurements are typical for these bands. Deviations of 10% are often encountered for the 7100-cm^{-1} band because its intensity is so low. In addition, background subtraction for this band in rhyolites is often difficult owing to the steep slope contributed to the background by Fe absorptions. The uncertainties in the absorbance measurements for the band at 4000 cm^{-1} are difficult to establish because its intensity is so dependent on the background-subtraction procedure; if the procedure described in Stolper (1982) is followed, uncertainties on the order of 0.01 absorbance units appear to be appropriate.

Water on polished surfaces. In view of the serious problems with surface-correlated water that we have documented in the course of our manometric analyses of hydrous glasses, we have paid close attention to the possibility that either adsorbed or absorbed water contributes to our IR spectra. Given the facts that we put a good polish on our samples and that the surface-area-to-volume ratios of our samples are very low, we did not expect that surface-correlated water would present any problems for us. Indeed, simple calculations show that neither a monolayer of water on the polished surfaces nor the amount of water that could hydrate our glasses on the time scale of years (Michels et al., 1983) could be detected, given the precision of our measurements. Nevertheless, we have been concerned about this problem and have conducted many tests to verify that it does not affect our spectra.

If surface-correlated water were a problem, one would expect that Beer's law would not hold; that is, the intensity of absorptions would not be proportional to sample thickness, since the amount of surface-correlated water would be independent of sample thickness. Figure 7 demonstrates that Beer's law does hold for the 3570-cm^{-1}, 4500-cm^{-1}, and 5200-cm^{-1} bands for glasses ranging in total water content from less than 100 ppm to greater than 1.7 wt% and verifies that surface water is not a problem for these samples.

We also compared the intensities of absorptions in samples of glass polished with diamond using oil as a lubricant against samples polished with alumina using water as a lubricant. No systematic differences were detected. Some samples polished under water had spectra obtained on them both before and after heating in vacuum at temperatures to greater than 100°C, and again, no differences were observed. Likewise, samples stored in the atmosphere for up to several years appear to neither gain nor lose water, on the basis of our spectroscopic measurements.

Although we have demonstrated that surface-correlated water is of negligible importance in the samples that we have studied, we believe that extreme care must be exercised during sample preparation and handling of specimens for IR analysis. For water-rich glasses with much higher diffusivities of water than the relatively water-poor samples that we have studied here or for alkali-rich compositions, water may be more readily absorbed from the environment or exuded from the sample.

Calibration of the IR technique—determination of molar absorptivities for the IR bands

Table 7 lists our preferred values for the molar absorptivities and integrated molar absorptivities in rhyolitic glasses for each of the absorption bands identified in this study. These parameters have been defined in terms of the amount of *water* that would be released from the sample if all of the hydrogen contributing to a given band were converted to H_2O. This definition of "molar absorptivity" allows the determination of the dissolved water content of a sample unambiguously and without danger of algebraic errors in converting the concentration of dissolved hydroxyl into the amount of water dissolved as hydroxyl. Surprisingly, there is much ambiguity in the literature about how molar absorptivities have been defined.

The concentration of dissolved "water" in a glass contributing to a given band can be determined as follows from the values given in Tables 5 and 6:

$$c = \frac{(18.02)(\text{abs})}{(\rho)(d)(\epsilon)}, \qquad (1)$$

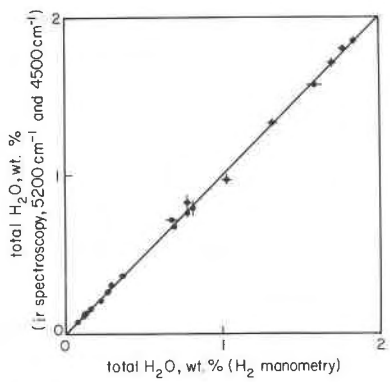

Fig. 8. Comparison between total water contents of glasses (1) determined by H_2 manometry and (2) based on summation of water dissolved as molecular water and hydroxyl groups determined by IR spectroscopy using molar absorptivities given in Table 7 for the 5200- and 4500-cm^{-1} bands. A 45° line, indicating perfect correspondence, is shown for comparison. Error bars for the IR measurements include errors in thickness, density, and absorbance measurements; the extinction coefficients were assumed to have no errors associated with them. Except for sample MC84-df, for which the two techniques deviate by 0.022 wt% (~3% of the amount present), the two techniques for measuring water content agree within calculated errors.

Table 7. Summary of molar absorptivities (ϵ) and integrated molar absorptivities (ϵ^*) for IR and NIR hydroxyl group and molecular water bands in rhyolitic glasses

Band (cm^{-1})	Species	ϵ [L/(mol·cm)]	ϵ^* [L/(mol·cm^2)]
7100	OH	0.320 ± 0.008	96**
	H_2O	0.184 ± 0.012	83**
5200	H_2O	1.61 ± 0.05	248 ± 24
4500	OH	1.73 ± 0.02	341 ± 25
4000	OH	1.14	290**
	H_2O	1.07	350**
3570	OH	100 ± 2	44 000 ± 1000
	H_2O	56 ± 4	26 300 ± 2200
1630	H_2O	55 ± 2	2640 ± 200

** Values uncertain owing to limited data and difficult background subtraction.

where c is the concentration in weight fraction, ρ is density given in g/L, d is thickness in centimeters, ϵ is the molar absorptivity in L/(mol·cm), and abs is absorbance, which is dimensionless. If integrated absorbance (cm^{-1}) is used instead of absorbance, ϵ is replaced by ϵ^*, the integrated molar absorptivity, with units of L/(mol·cm^2).

The parameters listed in Table 7 were determined via the following procedure: The first step was the determination of molar absorptivities for the molecular water band at 5200 cm^{-1} ($\epsilon_{H_2O,5200}$) and the hydroxyl group band at 4500 cm^{-1} ($\epsilon_{OH,4500}$). An equation was written giving total dissolved water as the sum of dissolved molecular water, based on the absorbance of the 5200-cm^{-1} band, and water dissolved as hydroxyl groups, based on the absorbance of the 4500-cm^{-1} band, for each of the 21 glasses for which the total water content was accurately known from H_2 manometric analysis. The molar absorptivities of the 5200-cm^{-1} and 4500-cm^{-1} bands were then determined on the basis of these 21 equations using a least-squares method similar to that given in Albarede and Provost (1977) by which errors could be assigned to all of the parameters given in Equation 1 and to the best-fit molar absorptivities. Only samples for which the manometric measurements and the spectroscopic measurements were carried out on the same glass fragment or on separate pieces from the same chunk of obsidian were included as part of this least-squares determination.

Our procedure for determining these molar absorptivities embodies two critical assumptions. First, molar absorptivities are assumed to be constant over the range of compositions studied. Second, all dissolved water is assumed to be present as either molecular water or as hydroxyl groups contributing to absorptions at 5200 cm^{-1} or 4500 cm^{-1}, respectively. The internal consistency of these assumptions can be tested by comparing total water contents obtained by summing spectroscopically determined molecular water and hydroxyl group water concentrations with the concentrations determined manometrically. Figure 8 shows this comparison and demonstrates that the extinction coefficients that we have determined are successful at recovering the manometrically determined water contents of the rhyolitic obsidians used to constrain them. If other forms of dissolved hydrogen that do not contribute to the bands at 5200 cm^{-1} or 4500 cm^{-1} are present in these glasses, they are either present in extremely small quantities or at a constant proportion of the total dissolved water content.

The integrated molar absorptivities for the 5200-cm^{-1} ($\epsilon^*_{H_2O,5200}$) and 4500-cm^{-1} ($\epsilon^*_{OH,4500}$) bands were determined by multiplying the value of the molar absorptivity times the average value of the ratio of the integrated absorbance to the absorbance for each band. We consider these integrated values to be less reliable than those based on straight peak heights because of uncertainties in the background-subtraction procedure.

The molar absorptivity of the fundamental H_2O band at 1630 cm^{-1} ($\epsilon_{H_2O,1630}$) was determined by finding the best-fit value of the ratio of the absorbance per unit thickness of the 1630-cm^{-1} band to the absorbance per unit thickness of the 5200-cm^{-1} band. The least-squares fit is displayed in Figure 9. Only the 19 samples for which the intensities of these two bands were measured on the same glass fragment or on pieces from the same fragment were used in determining this ratio. The excellent correspondence between the absorption coefficients for these two bands shown in Figure 9 is strong confirmation of our assignment of the 5200-cm^{-1} band to an H_2O-bending mode.

The integrated molar absorptivity of the band at 1630 cm^{-1} ($\epsilon^*_{H_2O,1630}$) given in Table 7 was calculated by multiplying the average ratio of the integrated absorbance to the absorbance for all rhyolitic glasses for which the intensity of this band was determined times $\epsilon_{H_2O,1630}$. Although this value is reasonably precise, its absolute value

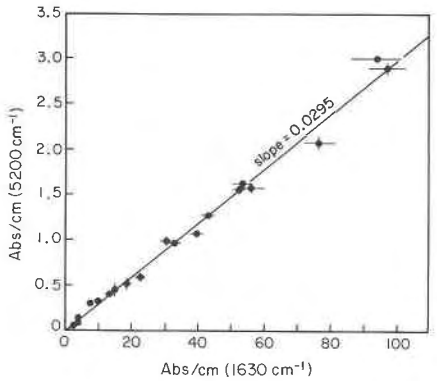

Fig. 9. Absorption coefficient of the 1630-cm^{-1} band versus that of the 5200-cm^{-1} band in rhyolitic glasses. A best-fit line, constrained to go through the origin, is shown for comparison. The excellent correspondence between the intensities of these bands supports the assignment of the 5200-cm^{-1} band to molecular water.

is rendered uncertain owing to the ambiguity in background subtraction for this band.

The molar absorptivity of the OH-stretch band at 3570 cm^{-1} decreases with increasing total dissolved water content. Both molecules of water and hydroxyl groups will contribute to this absorption; it would not be surprising if they had different molar absorptivities and thus that, as the ratio of molecular water to hydroxyl groups increases when the total water content increases (Stolper, 1982), the molar absorptivity of the 3570-cm^{-1} band would change from that of hydroxyl groups at low water contents

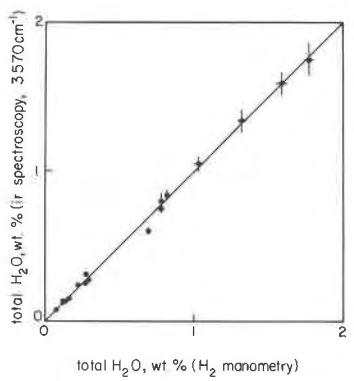

Fig. 10. Comparison between total water contents of glasses (1) determined by H_2 manometry and (2) determined by IR spectroscopy based on the intensity of the 3570-cm^{-1} OH-stretch band using the parameters given in Table 7. For most samples, the agreement between the two determinations is within error. Errors for the IR measurements include errors in absorbance, density, and thickness only. Deviations between the two determinations are typically less than 0.01–0.03 wt% H_2O; the maximum absolute deviation (0.096% H_2O) occurs for the sample MC84-df and corresponds to ~13% of the amount present. Note that the proportions of water dissolved as OH and H_2O must be known before the intensity of the 3570-cm^{-1} band can be used quantitatively (see text).

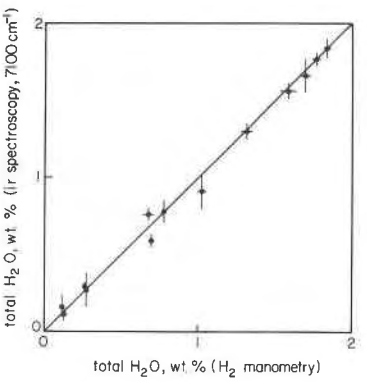

Fig. 11. Comparison between total water contents of glasses (1) determined by H_2 manometry and (2) determined by IR spectroscopy based on the intensity of the 7100-cm^{-1} OH-stretch band using the parameters given in Table 7. For all but one sample (MC84-df), the agreement is within error. Errors for the IR measurements include errors in absorbance, density, and thickness only. Note that the proportions of water dissolved as OH and H_2O must be known before the intensity of the 7100-cm^{-1} band can be used quantitatively (see text).

to some value intermediate between that of hydroxyl groups and that of molecules of water. Accordingly, we have modeled the intensity of the absorption at 3570 cm^{-1} as a combination of a contribution due to molecules of water and a contribution from hydroxyl groups, in which each species is assumed to have a constant molar absorptivity. For each of the 29 samples for which measurements of the intensities of the 5200-cm^{-1}, 4500-cm^{-1}, and 3570-cm^{-1} bands were made on the same fragment or on fragments from the same chunk of glass, an equation of the following sort was written:

$$\frac{\text{abs}_{3570}}{d_{\text{IR}}} = \frac{\text{abs}_{5200}\epsilon_{\text{H}_2\text{O},3570}}{d_{\text{NIR}}\epsilon_{5200}} + \frac{\text{abs}_{4500}\epsilon_{\text{OH},3570}}{d_{\text{NIR}}\epsilon_{4500}}, \tag{2}$$

where abs is absorbance and d_{IR} and d_{NIR} are the thicknesses of the fragments on which the absorbances of the 3570 cm^{-1} and of the two bands in the NIR were measured. $\epsilon_{\text{H}_2\text{O},3570}$ is the molar absorptivity of molecules of water at 3570 cm^{-1} and $\epsilon_{\text{OH},3570}$ is the molar absorptivity of hydroxyl groups at 3570 cm^{-1}. ϵ_{5200} and ϵ_{4500} are the molar absorptivities of the molecular water and hydroxyl group bands previously determined. The best-fit values of $\epsilon_{\text{H}_2\text{O},3570}/\epsilon_{5200}$ and $\epsilon_{\text{OH},3570}/\epsilon_{4500}$ were then determined by a least-squares procedure similar to that described in Albarede and Provost (1977). The values of $\epsilon_{\text{H}_2\text{O},3570}$ and $\epsilon_{\text{OH},3570}$ were then calculated from the values previously determined for ϵ_{5200} and ϵ_{4500}.

The value of the extinction coefficient for the 3570-cm^{-1} band is given by the following expression:

$$\epsilon_{3570} = X_{\text{OH}}\epsilon_{\text{OH},3570} + X_{\text{H}_2\text{O}}\epsilon_{\text{H}_2\text{O},3570}, \tag{3}$$

where X_{OH} and $X_{\text{H}_2\text{O}}$ are the fractions of water dissolved

in the glass as hydroxyl groups and molecules of water, respectively. The success of this procedure for modeling the extinction coefficient of the fundamental OH-stretch band can be evaluated by comparing total water contents determined manometrically with those calculated from the intensity of the 3570-cm^{-1} band using values for the extinction coefficient calculated using Equation 3 and values of X_{OH} and X_{H_2O} based on the intensities and molar absorptivities of the 4500-cm^{-1} and 5200-cm^{-1} bands. This comparison is shown in Figure 10. Although Figure 10 demonstrates that our simple model for the extinction coefficient of the 3570-cm^{-1} band is generally successful, the necessity that the speciation of water in a glass be known before an extinction coefficient for this band can be determined severely limits the utility of this band for measuring the water contents of glasses in which more than one species is dissolved.

Integrated molar absorptivities for molecules of water and hydroxyl groups for the 3570-cm^{-1} band were determined by an identical procedure to that described above for molar absorptivities. Their values, $\epsilon^*_{OH,3570}$ and $\epsilon^*_{H_2O,3570}$, are given in Table 7.

Like the band at 3570 cm^{-1}, its overtone at 7100 cm^{-1} has contributions from both water molecules and hydroxyl groups, and its extinction coefficient decreases with increasing water content. Accordingly, values for $\epsilon_{H_2O,7100}$ and $\epsilon_{OH,7100}$ were determined relative to the values for ϵ_{5200} and ϵ_{4500} by a procedure identical to that described above for the 3570-cm^{-1} band. Figure 11 compares water contents based on the intensity of the 7100-cm^{-1} band with values determined manometrically. The values typically agree within error. The poorer agreement observed in Figure 11 than in Figure 10 relates, we suspect, to the much lower intensity and consequent poorer precision of the absorbance measurements for the 7100-cm^{-1} band.

Values of the integrated molar absorptivities for the 7100-cm^{-1} band, $\epsilon^*_{OH,7100}$ and $\epsilon^*_{H_2O,7100}$, are not well constrained because very few integrated absorbances have been determined for this band and background-subtraction uncertainties are substantial. The values given in Table 7 are based on a ratio of ϵ^*_{7100} to ϵ_{7100} of 304 for sample DC-2 containing essentially no molecular water and a ratio of 330–370 for samples OBS-E, G, and I, containing both molecular water and hydroxyl in proportions determined from the 5200-cm^{-1} and 4500-cm^{-1} bands. We estimate uncertainties of perhaps as much as 15% for these ϵ^* values given in Table 7.

Molar absorptivity and integrated molar absorptivity for the 4000-cm^{-1} band were assumed, like the 3570-cm^{-1} and 7100-cm^{-1} bands, to have contributions both from molecular water and hydroxyl groups. Based on the results of Stolper (1982), it is clear that the suggestion of Acocella et al. (1984) that this band is due only to dissolved molecular water is not valid for rhyolitic glasses. This band is clearly present, and its intensity is approximately proportional to total dissolved water content in low-water glasses in which the concentration of molecular water is negligible, on the basis of the intensity of the 5200-cm^{-1} band. We have determined values for $\epsilon_{OH,4000}$ and $\epsilon_{H_2O,4000}$ and their integrated equivalents using the procedures described above for the 3570-cm^{-1} band. As emphasized above, however, the uncertainties in the background-subtraction procedure limit the reliability of these extinction coefficients and of measurements of dissolved water content based on this band.

We emphasize that only the extinction coefficients for the 5200-cm^{-1} and 4500-cm^{-1} band were determined directly from the manometric measurements of total water content. For all of the others, a best-fit value of the ratio of an extinction coefficient or an integrated extinction coefficient to one of these two values was determined. This procedure allowed us to utilize a much larger number of measurements in constraining these parameters since we have many absorbance measurements for samples for which total water contents were not manometrically determined. In addition, it will facilitate the updating and refinement of all of the extinction coefficients of interest as refinements of the 5200-cm^{-1} and 4500-cm^{-1} molar absorptivities become available.

Determination of water contents using IR spectroscopy—An evaluation

It is clear from Figures 8–11 that IR spectroscopy can provide precise and accurate measurements of total water contents of rhyolitic silicate glasses with up to 2 wt% dissolved water and of the concentrations of the different forms in which the water is dissolved. The precision comes from the availability of spectrometers that can accurately and reproducibly measure the intensities of absorption bands. The accuracy comes from the availability of suitable standards, in this case based on H_2 manometry, and from the apparent constancy of molar absorptivities over the narrow range of concentrations represented by the obsidians that we have studied.

The availability of suitable standards is critical to the application of IR spectroscopy for measuring water contents in glasses. The molar absorptivities reported in Table 7 differ from those reported by Stolper (1982). The reason is that in retrospect the water contents used for calibration purposes in that study were nearly all unreliable. Only when a series of standards all analyzed by a single, reliable technique is assembled can the limitations and potential of a technique such as IR spectroscopy be evaluated.

The large number of IR bands, with molar absorptivities ranging over almost three orders of magnitude, offers great flexibility for water analysis. Bands with high molar absorptivities such as the fundamental OH-stretch band at 3570 cm^{-1} are well suited for detecting very small quantities of water. For example, taking an absorbance of 0.03 as the detection limit, the detection limit for water in a 200-μm-thick piece of glass is 100 ppm. This can be reduced simply by using a thicker specimen. On the other hand, this band is poorly suited for studying water-rich specimens, both because the molar absorptivity is dependent on the relative proportions of molecular water and hydroxyl groups and because samples must be very thin

in order to keep absorbances from being so intense that they cannot be measured precisely. Bands in the NIR, particularly the bands at 5200 cm^{-1} and 4500 cm^{-1}, are well suited for precise determinations of total dissolved water contents of water-rich samples and have the added feature that species concentrations can be determined as well.

We emphasize that the molar absorptivities given in Table 7 only apply to rhyolitic glasses, and at this point we can only be confident of their applicability to glasses with up to about 2 wt% water. These parameters are definitely functions of the composition of the silicate portion of the glass (Stolper, 1982). We are encouraged, however, that this calibration is so well defined for this set of samples from diverse localities. The molar absorptivities could have been sensitive to the thermal histories of the glasses, to small variations in bulk chemistry, to total water content, or to other unknown parameters. This study has shown that the IR technique can be used quantitatively for determining water contents in a group of samples of similar chemistry but varying histories. Only after molar absorptivities have been systematically determined for a wider range of glass compositions based on reliable standards will we be able to assess how critical a knowledge of the major-element chemistry will be for precise determinations of water content by IR spectroscopy.

Conclusions

The two techniques discussed here can both yield precise determinations of total water content. They have different advantages and disadvantages and thus can be best utilized for different purposes. The vacuum extraction and manometry method is absolute, requires no calibration with standards of known water concentrations, and can be used to determine hydrogen isotopic compositions. With special precautions, only very small amounts of water (a few micromoles) are required for quantitative determinations (Yang and Epstein, 1983). However, the method is destructive in that the sample is melted and volatiles are lost. Another disadvantage is that relatively large sample sizes are required for precise analysis of glasses with low water contents.

The small sample size required by IR spectroscopy is one of this method's advantages. A large range of total water concentrations (from a few parts per million to tens of weight percent) can be determined on small samples and information on the forms of dissolved "water" (e.g., hydroxyl groups versus water molecules) can also be obtained. The infrared beam can be aimed at very small spots to study sample heterogeneity as well as to avoid phenocrysts, vesicles, and alteration. Since this method is nondestructive, a piece of glass can be analyzed by other techniques after infrared spectroscopy. The disadvantage is that it is not absolute and therefore must be calibrated against standards. This calibration must be done for each composition of interest, since molar absorptivities are dependent on major-element composition. The preparation of samples usually requires careful polishing and thickness control. In this paper we have presented a calibration for glasses of rhyolitic composition and thereby demonstrated that this technique is a valuable analytic tool. Prior to this study, we could not have been sure that small variations in glass chemistry, water content, or aspects of thermal history might not have resulted in sufficiently large variations in molar absorptivity that the IR technique would be of limited quantitative value.

Comparison of our manometric determinations of water content with determinations by other techniques dramatically demonstrates interlaboratory discrepancies in these measurements. We have shown that sample preparation can significantly affect water contents of crushed samples. Use of coarse powders is essential for correct determinations of concentration and δD values of water dissolved in rhyolite glasses. Temperatures on the order of 200°C are required to remove most of the surface-correlated water from fine-grained samples of low-water-content rhyolitic glasses. However, these temperatures may not be sufficient to extract all of the extraneous water from the most finely powdered samples (<75 μm); and they may be sufficient to begin the release of intrinsic, dissolved water.

Acknowledgments

The authors thank the following people for providing samples: A. T. Anderson, Jr., University of Chicago; I. S. E. Carmichael, University of California, Berkeley; T. Grove, Massachusetts Institute of Technology; K. Lapham, Arizona State University; H. Westrich, Sandia Laboratories; and M. Bursik and K. Sieh, California Institute of Technology. This study was supported by grant numbers EAR 83-3086 and EAR 84-17434 from the National Science Foundation and by DE-FG03-85ER13445 from the Department of Energy. This is contribution 4284 of the Division of Geological and Planetary Sciences, California Institute of Technology.

References

Acocella, J., Tomozawa, M., and Watson, E.B. (1984) The nature of dissolved water in silicate glasses and its effect on various properties. Journal of Non-Crystalline Solids, 65, 355–372.

Albarede, F., and Provost, A. (1977) Petrological and geochemical mass-balance equations: An algorithm for least-squares fitting and general error analysis. Computers and Geosciences, 3, 309–326.

Bartholomew, R.F., Butler, B.L., Hoover, H.L., and Wu, C.K. (1980) Infrared spectra of a water-containing glass. American Ceramic Society Journal, 63, 481–485.

Bryan, W.B., and Moore, J.G. (1977) Compositional variations of young basalts in the Mid-Atlantic Ridge rift valley near lat 36°49′N. Geological Society of America Bulletin, 88, 556–570.

Craig, H., and Lupton, J.E. (1976) Primordial neon, helium, and hydrogen in oceanic basalts. Earth and Planetary Science Letters, 31, 369–385.

Delaney, J.R., Muenow, D.W., and Graham, D.G. (1978) Abundance and distribution of water, carbon and sulfur in the glassy rims of submarine pillow basalts. Geochimica et Cosmochimica Acta, 42, 581–594.

Dushman, S. (1949) Scientific foundations of vacuum technique. Wiley, New York, 882 p.

Eichelberger, J.C., and Westrich, H.R. (1981) Magmatic volatiles in explosive rhyolitic eruptions. Geophysical Research Letters, 8, 757–760.

Epstein, S., and Taylor, H.P., Jr. (1970) The concentration and isotopic composition of hydrogen, carbon and silicon in Apollo

11 lunar rocks and minerals. Geochimica et Cosmochimica Acta Supplement 1, 2, 1085–1096.
Fine, G.J., and Stolper, E.M. (1985) The speciation of carbon dioxide in sodium aluminosilicate glasses. Contributions to Mineralogy and Petrology, 91, 105–121.
Friedman, I., and Long, W. (1976) Hydration rate of obsidian. Science, 191, 347–352.
Friedman, I., and Smith, R.L. (1958) The deuterium content of water in some volcanic glasses. Geochimica et Cosmochimica Acta, 15, 218–228.
Harris, D.M. (1981) The microdetermination of H_2O, CO_2, and SO_2 in glass using a 1280°C microscope vacuum heating stage, cryopumping, and vapor pressure measurements from 77 to 273 K. Geochimica et Cosmochimica Acta, 45, 2023–2036.
Harris, D.M., and Anderson, A.T., Jr. (1983) Concentrations, sources, and losses of H_2O, CO_2, and S in Kilauean basalt. Geochimica et Cosmochimica Acta, 47, 1139–1150.
——— (1984) Volatiles H_2O, CO_2, and Cl in a subduction related basalt. Contributions to Mineralogy and Petrology, 87, 120–128.
Jezek, P.A., and Noble, D.C. (1978) Natural hydration and ion exchange of obsidian: An electron microprobe study. American Mineralogist, 63, 266–273.
Killingley, J.S., and Muenow, D.W. (1975) Volatiles from Hawaiian submarine basalts determined by dynamic high temperature mass spectrometry. Geochimica et Cosmochimica Acta, 39, 1467–1473.
Knauth, L.P., and Epstein, S. (1982) The nature of water in hydrous silica. American Mineralogist, 67, 510–520.
Lee, R.R., Leich, D.A., Tombrello, T.A., Ericson, J.E., and Friedman, I. (1974) Obsidian hydration profile measurements using a nuclear reaction technique. Nature, 250, 44–47.
Michels, J.W., Tsong, I.S.T., and Nelson, C.M. (1983) Obsidian dating and East African archeology. Science, 219, 361–366.
Nakamoto, K. (1978) Infrared and Raman spectra of inorganic and coordination compounds, 3rd edition. Wiley, New York, 448 p.
Pineau, F., and Javoy, M. (1983) Carbon isotopes and concentrations in mid-oceanic ridge basalts. Earth and Planetary Science Letters, 62, 239–257.
Savitsky, A., and Golay, M.J.E. (1964) Smoothing and differentiation of data by simplified least squares procedures. Analytical Chemistry, 36, 1627–1639.
Scholze, H. (1960) Zur Frage der Unterscheidung zwischen H_2O-Molekeln und OH-Gruppen in Gläsern und Mineralen. Naturwissenschaften, 47, 226–227.
——— (1966) Gases and water in glass. Glass Industry, 47, 546–551, 622–628.
Shaw, H.R. (1974) Diffusion of H_2O in granitic liquid. I. Experimental data. II. Mass transfer in magma chambers. In A.W. Hoffmann, B.J. Giletti, H.S. Yoder, Jr., and R.A. Yund, Eds. Geochemical transport and kinetics, 139–170. Carnegie Institution of Washington Publications, 634.
Stolper, E. (1982) Water in silicate glasses: An infrared spectroscopic study. Contributions to Mineralogy and Petrology, 81, 1–17.
Taylor, B.E., Eichelberger, J.C., and Westrich, H.R. (1983) Hydrogen isotopic evidence of rhyolitic magma degassing during shallow intrusion and eruption. Nature, 306, 541–545.
Wu, C.-K. (1980) Nature of incorporated water in hydrated silicate glasses. American Ceramic Society Journal, 63, 453–457.
Yang, J., and Epstein, S. (1983) Interstellar organic matter in meteorites. Geochimica et Cosmochimica Acta, 47, 2199–2216.

Manuscript received December 24, 1985
Manuscript accepted July 8,1986